PERGAMON

International Journal of Heat and Mass Transfer 45 (2002) 2509–2525

International Journal of HEAT and MASS TRANSFER

www.elsevier.com/locate/ijhmt

On laminar hydromagnetic mixed convection flow in a vertical channel with symmetric and asymmetric wall heating conditions

Ali J. Chamkha *

Mechanical Engineering Department, Kuwait University, P.O. Box 5969, Safat 13060, Kuwait

Received 8 February 2000; received in revised form 1 November 2001

Abstract

The problem of hydromagnetic fully developed laminar mixed convection flow in a vertical channel with symmetric and asymmetric wall heating conditions in the presence or absence of heat generation or absorption effects is considered. Through proper choice of dimensionless variables, the governing equations are developed and three types of thermal boundary conditions are prescribed. These thermal boundary conditions are isothermal–isothermal, isoflux–isothermal, and isothermal–isoflux for the left–right walls of the channel. Analytical solutions for the velocity and temperature profiles for various special cases of the problem are reported. In addition, closed-form expressions for the Nusselt numbers and reversal flow conditions at both the left and right channel walls are derived. The general problem which includes the effects of both viscous dissipation and Joule heating is solved numerically by an implicit finite-difference scheme. Favorable comparisons of special cases with previously published work are obtained. A selected set of graphical results illustrating the effects of the various parameters involved in the problem including viscous and magnetic dissipations on the velocity and temperature profiles as well as flow reversal situations and Nusselt numbers is presented and discussed. © 2002 Published by Elsevier Science Ltd.

1. Introduction

Mixed convection flow in a vertical channel has been the subject of many previous investigations due its possible application in many industrial and engineering processes. These include cooling of electronic equipment, heating of the Trombe wall system, gas-cooled nuclear reactors and others. Tao [17] analyzed laminar fully developed mixed convection flow in a vertical parallel-plate channel with uniform wall temperatures. Aung and Worku [1,2] discussed the theory of combined free and forced convection in a vertical channel with flow reversal conditions for both developing and fully developed flows. Aung and Worku [2] assumed that the walls of the channel were having asymmetric temperatures. The case of developing mixed convection flow in ducts with asymmetric wall heat fluxes was analyzed by the same authors [3]. A comprehensive review of the literature dealing with mixed convection in internal flow was reported by Aung [4]. Cheng et al. [9], Hamadah and Wirtz [11] and Ingham et al. [12] also reported on flow reversal situations in mixed convection in a vertical channel for different wall heating conditions. Kou and Lu [13] analyzed mixed convection in a porous medium channel and discussed the conditions for flow reversal situations.

The use of electrically conducting fluids under the influence of magnetic fields in various industries has led to a renewed interest in investigating hydromagnetic flow and heat transfer in different geoemetries. For example, Sparrow and Cess [15] considered the effect of a magnetic field on the free convection heat transfer from a surface. Raptis and Kafoussias [14]

* Tel.: +965-571-2298; fax: +965-484-7131.

E-mail address: chamkha@kuc01.kuniv.edu (A.J. Chamkha).

0017-9310/02/$ - see front matter © 2002 Published by Elsevier Science Ltd.
PII: S0017-9310(01)00342-8

Nomenclature

A	constant pressure gradient (Pa m^{-1})
B_0	magnetic induction (tesla)
Br	Brinkman number defined in Eq. (7)
c	specific heat at constant pressure (J kg^{-1} K^{-1})
D	$=2L$, hydraulic diameter (m)
Gr	Grashof number defined in Eq. (7)
h_1, h_2	heat transfer coefficients at left and right walls, respectively (W m^{-2} K^{-1})
g	acceleration due to gravity (m s^{-2})
k	thermal conductivity (W m^{-1} K^{-1})
L	channel width (m)
M	Hartmann number defined in Eq. (7)
Nu_1, Nu_2	Nusselt numbers defined by Eqs. (69), (73) or (78)
p	pressure (Pa)
P	$=p+\rho gx$, difference between the pressure and the hydrostatic pressure (Pa)
Pr	Prandtl number defined in Eq. (7)
q_1, q_2	prescribed boundary heat fluxes per unit area (W m^{-2})
Q_0	heat generation, or absorption, coefficient (W m^{-3} K^{-1})
Re	Reynolds number defined in Eq. (7)
R_t	$=(T_2-T_1)/\Delta T$, temperature difference ratio
R_{qt}	$=(T_2-T_0)/\Delta T$, thermal ratio parameter
R_{tq}	$=(T_1-T_0)/\Delta T$, thermal ratio parameter
T	temperature (K)
T_1, T_2	prescribed boundary temperatures (K)
T_0	reference ambient temperature, $=(T_1+T_2)/2$, (K) for isothermal walls
u	dimensional velocity component in the x-direction (m s^{-1})
u_0	$=AD^2/(48\mu)$, reference velocity (m s^{-1})
U	dimensionless velocity component in the x-direction
x	streamwise coordinate (m)
y	transverse coordinate (m)

Greek symbols

α	$=k/(\rho c)$, thermal diffusivity (m^2 s^{-1})
β	thermal expansion coefficient (K^{-1})
ΔT	reference temperature difference (K)
η	dimensionless transverse coordinate defined in Eq. (7)
ϕ	dimensionless heat generation or absorption coefficient defined in Eq. (7)
θ	dimensionless temperature defined by Eq. (7)
μ	dynamic viscosity (Pa s)
v	$=\mu/\rho$, kinematic viscosity (m^2 s^{-1})
ρ	fluid density (kg m^3)
σ	fluid electrical conductivity (mho m^{-1})

analyzed flow and heat transfer through a porous medium bounded by an infinite vertical plate under the action of a magnetic field. Garandet et al. [10] discussed buoyancy driven convection in a rectangular enclosure with a transverse magnetic field. Chamkha [7] analyzed free convection effects on three-dimensional flow over a vertical stretching surface in the presence of a magnetic field.

The study of internal heat generation or absorption in moving fluids is important in view of several physical problems such as those dealing with chemical reactions and those concerned with dissociating fluids (see, for instance, [18,19]). Other investigations dealing with internal heat generation or absorption can be found in the works of Sparrow and Cess [16] and Chamkha [7].

The aim of the present work is to extend studies available in the literature and especially the work of Barletta [5] on laminar fully developed mixed convection in a vertical parallel-plate channel by including internal heat generation or absorption and magnetic field effects. This will be done for three types of left–right walls thermal conditions. These conditions are the isothermal–isothermal, isoflux–isothermal and the isothermal–isoflux thermal wall conditions.

2. Governing equations

Consider steady laminar mixed convective flow in a parallel-plate vertical channel in the presence of a magnetic field and a heat source or sink. The vertical plates are separated by a distance L and are maintained at either constant temperature or constant heat flux (see Fig. 1). Let x and y represent the vertical and horizontal distances, respectively, with the origin being at the center of the channel. Let the magnetic field be applied in the horizontal direction normal to the flow direction. The working fluid is assumed to be Newtonian, electrically conducting, and heat generating or absorbing and its properties are assumed constant except the density in the body force term of the momentum equation. Also, it is assumed that x-component of velocity is the only non-zero component. Under the above assumptions and by invoking the Boussinesq approximation, the governing equations can be written as:

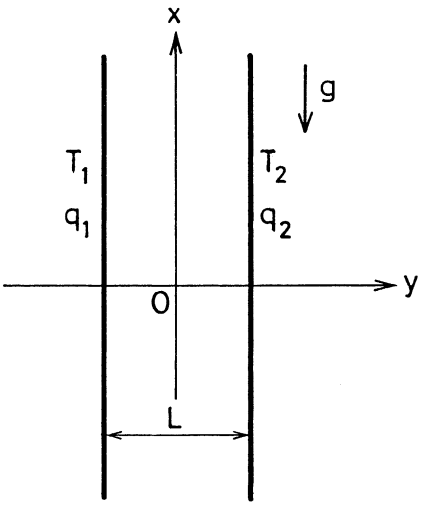

Fig. 1. Problem schematics and coordinate system.

$$\frac{\partial u}{\partial x}=0, \tag{1}$$

$$u\frac{\partial u}{\partial x}=-\frac{1}{\rho}\frac{\mathrm{d}P}{\mathrm{d}x}+\beta g(T-T_0)+\nu\frac{\partial^2 u}{\partial y^2}-\frac{\sigma B_0^2 u}{\rho}, \tag{2}$$

$$u\frac{\partial T}{\partial x}=\frac{k}{\rho c}\frac{\partial^2 T}{\partial y^2}+\frac{\mu}{\rho c}\left(\frac{\partial u}{\partial y}\right)^2+\frac{\sigma B_0^2}{\rho c}u^2\pm\frac{Q_0}{\rho c}(T-T_0), \tag{3}$$

where u and T are the x-component of velocity and temperature, respectively, $P=p+\rho gx$ is the difference between the pressure and hydrostatic pressure. ρ, μ, ν, k and c are the fluid density, dynamic viscosity, kinematic viscosity, thermal conductivity and specific heat at constant pressure, respectively. β, g, σ, B_0, and Q_0 are the thermal expansion coefficient, gravitational acceleration, fluid electrical conductivity, magnetic induction, and the heat generation or absorption coefficient, respectively. T_0 is a reference ambient temperature. In the proceeding sections, it will be necessary to distinguish between heat generation cases and heat absorption cases because a general solution in which Q_0 can be either positive or negative experiences difficulties upon numerical evaluation such as the evaluation of complex numbers, etc. For this reason, the positive or negative signs in front of the last term of Eq. (3) are used such that the positive sign indicates heat generation and the negative sign indicates heat absorption. In this way, $Q_0>0$ for both situations.

Eq. (1) suggests that u will only be a function of the horizontal distance y. Also for the three different wall heating conditions of isothermal–isothermal, isoflux–isothermal and isothermal–isoflux, a constant pressure gradient ($\mathrm{d}P/\mathrm{d}x=A$) is required for the compatibility with Eq. (2). Taking these facts into consideration and differentiating Eq. (2) with respect to x gives

$$\frac{\partial T}{\partial x}=0. \tag{4}$$

Eq. (4) indicates that the temperature is also a function of y only.

Combining the remaining terms of both Eqs. (2) and (3) gives

$$u^{\mathrm{IV}}-\left(\frac{\sigma B_0^2}{\rho\nu}\mp\frac{Q_0}{k}\right)u''\mp\frac{Q_0}{k}\frac{\sigma B_0^2}{\rho\nu}u\mp\frac{Q_0}{k}\frac{A}{\rho\nu}-\frac{\rho\beta g}{k}(u')^2-\frac{\sigma B_0^2\beta g}{k\nu}u^2=0, \tag{5}$$

where a prime denotes ordinary differentiation with respect to y.

Four boundary conditions for u are needed to solve Eq. (5). These are the two no-slip conditions at both walls and the other two induced by the thermal boundary conditions which can be obtained from evaluating Eq. (2) at each wall. Therefore, the boundary conditions for the case of isothermal–isothermal (T_1-T_2) walls can be written as

$$\begin{aligned}&u\left(-\frac{L}{2}\right)=0,\quad u\left(\frac{L}{2}\right)=0,\\ &u''\left(-\frac{L}{2}\right)=\frac{A}{\mu}-\frac{\beta g(T_1-T_0)}{\nu}+\frac{\sigma B_0^2}{\mu}u\left(-\frac{L}{2}\right),\\ &u''\left(\frac{L}{2}\right)=\frac{A}{\mu}-\frac{\beta g(T_2-T_0)}{\nu}+\frac{\sigma B_0^2}{\mu}u\left(\frac{L}{2}\right).\end{aligned} \tag{6}$$

Eqs. (5) and (6) can be written in dimensionless form by employing the dimensionless quantities given earlier by Barletta [5]

$$\begin{aligned}&\eta=\frac{y}{D},\quad U=\frac{u}{u_0},\quad \theta=\frac{T-T_0}{\Delta T},\\ &Gr=\frac{g\beta\Delta TD^3}{\nu^2},\quad M^2=\frac{\sigma B_0^2}{\mu}D^2,\quad Re=\frac{u_0\mathrm{D}}{\nu},\\ &Pr=\frac{\mu c}{k},\quad Br=\frac{\mu u_0^2}{k\Delta T},\quad \phi=\frac{Q_0D^2}{k}\end{aligned} \tag{7}$$

(where $u_0=AD^2/(48\mu)$ is a reference velocity, ΔT is a reference temperature difference which is different for different wall thermal boundary conditions, and $D=2L$ is the hydraulic diameter) to yield

$$U^{\mathrm{IV}}-(M^2\mp\phi)U''\mp M^2\phi U-\frac{Gr}{Re}Br(U')^2-\frac{Gr}{Re}BrM^2U^2\pm48\phi=0, \tag{8}$$

$$\begin{aligned}&U\left(-\frac{1}{4}\right)=0,\quad U\left(\frac{1}{4}\right)=0,\\ &U''\left(-\frac{1}{4}\right)=-48+\frac{R_t}{2}\frac{Gr}{Re},\\ &U''\left(\frac{1}{4}\right)=-48-\frac{R_t}{2}\frac{Gr}{Re},\end{aligned} \tag{9}$$

where a prime in Eq. (8) denotes ordinary differentiation with respect to η and $R_t = (T_2 - T_1)/\Delta T$ is a thermal ratio parameter for the isothermal–isothermal case.

As a consequence of Eqs. (2), (3) and (8), the dimensionless temperature can, be determined from the equation:

$$\theta = -\frac{1}{Gr/Re}(48 + U'' - M^2 U). \tag{10}$$

It is worth, noting here that for the case of isothermal walls $T_0 = (T_1 + T_2)/2$ and $\Delta T = T_2 - T_1$ if $T_1 < T_2$ (asymmetric wall heating) or $\Delta T = v^2/(cD^2)$ if $T_1 = T_2$ (symmetric wall heating). As a consequence of this, $R_t = 0$ for the symmetric wall heating case and $R_t = 1$ for the asymmetric wall heating case.

3. Analytical solutions

Various analytical solutions for special cases of the problem described above are possible only in the absence of both viscous and magnetic dissipation terms. These are reported for the following nine special cases:

Case 1. Hydromagnetic mixed convection flow in a vertical channel with isothermal walls.

For this special case the viscous and magnetic dissipations and the heat generation or absorption effect are neglected ($Br = 0$ and $\phi = 0$). Using this, Eq. (8) reduces to

$$U^{IV} - M^2 U'' = 0. \tag{11}$$

Solution of Eq. (11) subject to Eqs. (9) can be shown to yield

$$U = \frac{C_1}{M^2}\sinh(M\eta) + \frac{C_2}{M^2}\cosh(M\eta) + C_3\eta + C_4, \tag{12}$$

where

$$C_1 = -\frac{R_t Gr}{2Re}\operatorname{csch}\left(\frac{M}{4}\right), \quad C_2 = -48\operatorname{sech}\left(\frac{M}{4}\right), \quad C_3 = \frac{2R_t}{M^2}\frac{Gr}{Re}, \quad C_4 = \frac{48}{M^2}. \tag{13}$$

With U being known, the temperature distribution in the channel can be found from Eq. (10). This can be shown to be

$$\theta = 2R_t\eta, \tag{14}$$

which is the solution reported earlier by Barletta [5].

Case 2. Mixed convection flow in a vertical channel with isothermal walls in the presence of a heat source or sink.

For the titled problem $Br = 0$ and $M = 0$. For this situation Eq. (8) reduces to

$$U^{IV} + \phi U'' = -48\phi \tag{15}$$

for the case of heat generation and

$$U^{IV} - \phi U'' = 48\phi \tag{16}$$

for the case of heat absorption.

Without going into detail, it can be shown that the solutions of Eqs. (15) and (16) subject to Eqs. (9) can, respectively, be written as

$$U = C_5\sin(\sqrt{\phi}\eta) - 24\eta^2 - \frac{2R_t}{\phi}\frac{Gr}{Re}\eta + \frac{3}{2}, \tag{17}$$

$$U = C_6\sinh(\sqrt{\phi}\eta) - 24\eta^2 + \frac{2R_t}{\phi}\frac{Gr}{Re}\eta + \frac{3}{2}, \tag{18}$$

where

$$C_5 = \frac{R_t Gr/Re}{2\phi\sin(\sqrt{\phi}/4)}, \quad C_6 = \frac{R_t Gr/Re}{2\phi\sinh(\sqrt{\phi}/4)}. \tag{19}$$

The corresponding temperature distributions for the heat generation and heat absorption cases can, respectively, be written as

$$\theta = \frac{C_5\phi}{Gr/Re}\sin(\sqrt{\phi}\eta), \tag{20}$$

$$\theta = -\frac{C_6\phi}{Gr/Re}\sinh(\sqrt{\phi}\eta). \tag{21}$$

It can be shown that as $\phi \to 0$, the solutions for U and θ approach those reported by Barletta [5].

Case 3. Hydromagnetic mixed convection flow in a vertical channel with isothermal walls in the presence of a heat source or sink.

For this special case, setting $Br = 0$ in Eq. (8) yields

$$U^{IV} - (M^2 - \phi)U'' - M^2\phi U + 48\phi = 0 \tag{22}$$

for the case of heat generation and

$$U^{IV} - (M^2 + \phi)U'' + M^2\phi U - 48\phi = 0 \tag{23}$$

for the case of heat absorption.

Again, without going into detail, the solutions for the velocity and temperature distributions (U and θ) in the channel can be written as

$$U = C_7\sinh(M\eta) + C_8\cosh(M\eta) + C_9\sin(\sqrt{\phi}\eta) + \frac{48}{M^2}, \tag{24}$$

$$\theta = \frac{C_9(\phi + M^2)\sin(\sqrt{\phi}\eta)}{Gr/Re} \tag{25}$$

for the heat generation case and

$$U = C_{10}\sinh(M\eta) + C_8\cosh(M\eta) + C_{11}\sinh(\sqrt{\phi}\eta) + \frac{48}{M^2}, \tag{26}$$

$$\theta = -\frac{C_{11}(\phi - M^2)\sinh(\sqrt{\phi}\eta)}{Gr/Re}, \tag{27}$$

where

$$C_7 = -\frac{R_t Gr/Re}{2(M^2+\phi)\sinh(M/4)},$$
$$C_8 = -\frac{48}{M^2\cosh(M/4)},$$
$$C_9 = \frac{R_t Gr/Re}{2(M^2+\phi)\sin(\sqrt{\phi}/4)}, \quad (28)$$
$$C_{10} = -\frac{R_t Gr/Re}{2(M^2-\phi)\sinh(M/4)},$$
$$C_{11} = \frac{-R_t Gr/Re}{2(\phi-M^2)\sinh(\sqrt{\phi}/4).}$$

Isoflux–isothermal walls ($q_1 - T_2$)

For this situation, the thermal boundary conditions for the channel walls can be written in the dimensional form as

$$q_1 = -k\left.\frac{dT}{dy}\right|_{-L/2}, \quad T(L/2) = T_2. \quad (30)$$

The dimensionless form of Eqs. (30) can be obtained by using Eqs. (7) with $\Delta T = q_1 D/k$ to give

$$\theta'\left(-\frac{1}{4}\right) = -1, \quad \theta\left(\frac{1}{4}\right) = R_{qt}, \quad (31)$$

where $R_{qt} = (T_2 - T_0)/\Delta T$ is the thermal ratio parameter for the isoflux–isothermal case.

Other than the no-slip conditions at the channel walls, two more boundary conditions in terms of u are needed to solve Eq. (8) for this case. These are induced by the conditions given in Eqs. (30) and are obtained from Eq. (2) as follows:

Differentiating Eq. (2) with respect to y with $dP/dx = A$ gives

$$u''' - \frac{\sigma B_0^2}{\mu}u' + \frac{\beta g}{\nu}T' = 0. \quad (32)$$

Eq. (32) is non-dimensionalized by using Eqs. (7) to give

$$U''' - M^2 U' + \frac{Gr}{Re}.\theta' = 0. \quad (33)$$

Evaluating Eq. (33) at the left walls ($\eta = -1/4$) yields

$$U'''(-1/4) - M^2 U'(-1/4) = \frac{Gr}{Re}. \quad (34)$$

The other boundary condition at the right wall can be shown to be the same as that given for the isothermal–isothermal case with R_t replaced by R_{qt} such that

$$U''(1/4) = -48 - \frac{R_{qt}}{2}\frac{Gr}{Re}. \quad (35)$$

Case 4. Hydromagnetic mixed convection flow in a vertical channel with isoflux–isothermal walls.

In the absence of both viscous and magnetic dissipations ($Br = 0$) and heat generation or absorption ($\phi = 0$), the analytical solutions for the velocity and temperature distributions are obtained by solving of Eqs. (8) and (10) subject to Eqs. (34) and (35) and the no-slip conditions at the wall. These solutions can be shown to be

$$U = \frac{C_{12}}{M^2}\sinh(M\eta) + \frac{C_{13}}{M^2}\cosh(M\eta) + C_{14}\eta + C_{15}, \quad (36)$$

$$\theta = \frac{M^2}{Gr/Re}[C_{14}\eta + C_{15}], \quad (37)$$

where

$$C_{12} = \frac{1}{4}\frac{Gr}{Re}\operatorname{csch}\left(\frac{M}{4}\right), \quad C_{13} = -\frac{48 + Gr/Re(1/4 + R_{qt})}{\cosh(M/4)},$$
$$C_{14} = -\frac{Gr}{ReM^2}, \quad C_{15} = \frac{48 + Gr/Re(1/4 + R_{qt})}{M^2} \quad (38)$$

Case 5. Mixed convection flow in a vertical channel with isoflux–isothermal walls in the presence of a heat source or sink.

The solutions for the velocity and temperature distributions for this case are obtained in a similar way as its isothermal–isothermal counterpart but with the use of Eqs. (34) and (35) instead of the last two conditions of Eqs. (9). The velocity and temperature distributions can be shown to be

$$U = C_{16}\sin(\sqrt{\phi}\eta) + C_{17}\cos(\sqrt{\phi}\eta) - 24\eta^2 + C_{18}\eta + C_{19}, \quad (39)$$

$$\theta = \frac{\phi}{Gr/Re}[C_{16}\sin(\sqrt{\phi}\eta) + C_{17}\cos(\sqrt{\phi}\eta)], \quad (40)$$

where

$$C_{16} = -\frac{Gr/Re[\cos(\sqrt{\phi}/4) + \sqrt{\phi}R_{qt}\sin(\sqrt{\phi}/4)]}{\phi^{3/2}\cos(\sqrt{\phi}/2)},$$
$$C_{17} = \frac{Gr/Re[\sin(\sqrt{\phi}/4) + \sqrt{\phi}R_{qt}\cos(\sqrt{\phi}/4)]}{\phi^{3/2}\cos(\sqrt{\phi}/2)}, \quad (41)$$
$$C_{18} = -4C_{16}\sin(\sqrt{\phi}/4),$$
$$C_{19} = \frac{3}{2} - C_{17}\cos(\sqrt{\phi}/4)$$

for the heat generation case and

$$U = C_{20}\sinh(\sqrt{\phi}\eta) + C_{21}\cosh(\sqrt{\phi}\eta) - 24\eta^2 + C_{22}\eta + C_{23}, \quad (42)$$

$$\theta = \frac{-\phi}{Gr/Re}[C_{20}\sinh(\sqrt{\phi}\eta) + C_{21}\cosh(\sqrt{\phi}\eta)], \quad (43)$$

where

$$C_{20}=\frac{Gr/Re[\cosh(\sqrt{\phi}/4)-R_{qt}\sqrt{\phi}\sinh(\sqrt{\phi}/4)]}{\phi^{3/2}\cosh(\sqrt{\phi}/2)},$$
$$C_{21}=\frac{-Gr/Re[\sinh(\sqrt{\phi}/4)+R_{qt}\sqrt{\phi}\cosh(\sqrt{\phi}/4)]}{\phi^{3/2}\cosh(\sqrt{\phi}/2)},$$
$$C_{22}=-4C_{20}\sinh(\sqrt{\phi}/4),\quad C_{23}=\frac{3}{2}-C_{21}\cosh(\sqrt{\phi}/4) \tag{44}$$

for the heat absorption case.

Case 6. Hydromagnetic mixed convection flow in a vertical channel with isoflux–isothermal walls in the presence of a heat source or sink.

This problem is the isoflux–isothermal counterpart of the problem for isothermal–isothermal walls. Therefore, the method of solution is the same except the boundary conditions (34) and (35) are used instead of the last conditions of Eqs. (9). The general solutions for U and θ associated, with this problem can be shown to be

$$U=C_{24}\sinh(M\eta)+C_{25}\cosh(M\eta)+C_{26}\sin(\sqrt{\phi}\eta)+C_{27}\cos(\sqrt{\phi}\eta)+\frac{48}{M^2}, \tag{45}$$

$$\theta=\frac{(\phi+M^2)}{Gr/Re}[C_{26}\sin(\sqrt{\phi}\eta)+C_{27}\cos(\sqrt{\phi}\eta)], \tag{46}$$

where

$$C_{24}=-\frac{C_{26}\sin(\sqrt{\phi}/4)}{\sinh(M/4)},$$
$$C_{25}=\frac{-48/M^2-C_{27}\cos(\sqrt{\phi}/4)}{\cosh(M/4)},$$
$$C_{26}=\frac{-Gr/Re[R_{qt}\sqrt{\phi}\sin(\sqrt{\phi}/4)+\cos(\sqrt{\phi}/4)]}{\sqrt{\phi}(M^2+\phi)\cos(\sqrt{\phi}/2)},$$
$$C_{27}=\frac{Gr/Re[R_{qt}\sqrt{\phi}\cos(\sqrt{\phi}/4)+\sin(\sqrt{\phi}/4)]}{\sqrt{\phi}(M^2+\phi)\cos(\sqrt{\phi}/2)} \tag{47}$$

for the heat generation case and

$$U=C_{28}\sinh(M\eta)+C_{29}\cosh(M\eta)+C_{30}\sinh(\sqrt{\phi}\eta)+C_{31}\cosh(\sqrt{\phi}\eta)+\frac{48}{M^2}, \tag{48}$$

$$\theta=\frac{-(\phi-M^2)}{Gr/Re}[C_{30}\sinh(\sqrt{\phi}\eta)+C_{31}\cosh(\sqrt{\phi}\eta)], \tag{49}$$

where

$$C_{28}=-\frac{C_{30}\sinh(\sqrt{\phi}/4)}{\sinh(M/4)},$$
$$C_{29}=\frac{-48/M^2-C_{31}\cosh(\sqrt{\phi}/4)}{\cosh(M/4)},$$
$$C_{30}=\frac{Gr/Re[\cosh(\sqrt{\phi}/4)-R_{qt}\sqrt{\phi}\sinh(\sqrt{\phi}/4)]}{\sqrt{\phi}(\phi-M^2)\cosh(\sqrt{\phi}/2)},$$
$$C_{31}=\frac{-Gr/Re[\sinh(\sqrt{\phi}/4)+R_{qt}\sqrt{\phi}\cosh(\sqrt{\phi}/4)]}{\sqrt{\phi}(\phi-M^2)\cosh(\sqrt{\phi}/2)} \tag{50}$$

for the heat absorption case.

Isothermal–isoflux walls (T_1-q_2)

The dimensional form of the thermal boundary conditions for this case can be written as

$$T(-L/2)=T_1,\quad q_2=-k\left.\frac{dT}{dy}\right|_{L/2}, \tag{51}$$

where q_2 is a constant. Eqs. (51) can be made dimensionless by using Eqs. (7) with $\Delta T=q_2D/k$. This can be shown to give

$$\theta(-1/4)=R_{tq},\quad \theta'(1/4)=-1, \tag{52}$$

where $R_{tq}=(T_1-T_0)/\Delta T$ is the thermal ratio parameter for the isothermal–isoflux case.

Similar to the procedure done in the previous section on isoflux–isothermal walls, the dimensionless form of the boundary conditions obtained from using Eq. (2) and applying Eq. (52) can be written as

$$U''(-1/4)=-48-R_{tq}\frac{Gr}{Re},$$
$$U'''(1/4)-M^2U'(1/4)=\frac{Gr}{Re}. \tag{53}$$

Case 7. Hydromagnetic mixed convection flow in a vertical channel with isothermal–isoflux walls.

For the above titled problem with $Br=0$ and $\phi=0$, the velocity and temperature distributions in the vertical channel can be shown to be

$$U=\frac{C_{32}}{M^2}\sinh(M\eta)+\frac{C_{33}}{M^2}\cosh(M\eta)+C_{34}\eta+C_{35}, \tag{54}$$

$$\theta=\frac{1}{Gr/Re}[M^2(C_{34}\eta+C_{35})-48], \tag{55}$$

where

$$C_{32}=\frac{1}{4}\frac{Gr}{Re}\operatorname{csch}\left(\frac{M}{4}\right),$$
$$C_{33}=\frac{-48-Gr/Re(R_{tq}-1/4)}{\cosh(M/4)},$$
$$C_{34}=-\frac{Gr}{ReM^2},$$
$$C_{35}=\frac{48+Gr/Re(R_{tq}-1/4)}{M^2}. \tag{56}$$

Case 8. Mixed convection flow in a vertical channel with isothermal–isoflux walls in the presence of a heat source or sink.

In the absence of the magnetic field ($M=0$) and both of the viscous and magnetic dissipations, solution of Eqs. (8) and (10) subject to Eqs. (53) and the first two conditions of Eqs. (9) yields

$$U=C_{36}\sin(\sqrt{\phi}\eta)+C_{37}\cos(\sqrt{\phi}\eta)-24\eta^2+C_{38}\eta+C_{39}, \tag{57}$$

$$\theta=\frac{\phi}{Gr/Re}[C_{36}\sin(\sqrt{\phi}\eta)+C_{37}\cos(\sqrt{\phi}\eta)], \tag{58}$$

where

$$C_{36} = -\frac{Gr/Re[\cos(\sqrt{\phi}/4) - R_{tq}\sqrt{\phi}\sin(\sqrt{\phi}/4)]}{\phi^{3/2}\cos(\sqrt{\phi}/2)},$$
$$C_{37} = -\frac{Gr/Re[\sin(\sqrt{\phi}/4) - R_{tq}\sqrt{\phi}\cos(\sqrt{\phi}/4)]}{\phi^{3/2}\cos(\sqrt{\phi}/4)}, \quad (59)$$
$$C_{38} = -4C_{36}\sin(\sqrt{\phi}/4),$$
$$C_{39} = \frac{3}{2} - C_{37}\cos(\sqrt{\phi}/4)$$

for the heat generation case and

$$U = C_{40}\sinh(\sqrt{\phi}\eta) + C_{41}\cosh(\sqrt{\phi}\eta) - 24\eta^2 + C_{42}\eta + C_{43}, \quad (60)$$

$$\theta = \frac{-\phi}{Gr/Re}[C_{40}\sinh(\sqrt{\phi}\eta) + C_{41}\cosh(\sqrt{\phi}\eta)], \quad (61)$$

where

$$C_{40} = \frac{Gr/Re[\cosh(\sqrt{\phi}/4) + R_{tq}\sqrt{\phi}\sinh(\sqrt{\phi}/4)]}{\phi^{3/2}\cosh(\sqrt{\phi}/2)},$$
$$C_{41} = \frac{Gr/Re[\sinh(\sqrt{\phi}/4) - R_{tq}\sqrt{\phi}\cosh(\sqrt{\phi}/4)]}{\phi^{3/2}\cosh(\sqrt{\phi}/2)}, \quad (62)$$
$$C_{42} = -4C_{40}\sinh(\sqrt{\phi}/4),$$
$$C_{43} = \frac{3}{2} - C_{41}\cosh(\sqrt{\phi}/4)$$

for the heat absorption case.

Case 9. Hydromagnetic mixed convection flow in a vertical channel with isothermal–isoflux walls in the presence of a heat source or sink.

The analytical solutions for the velocity and temperature profiles within the vertical channel for this case can be shown to be

$$U = C_{44}\sinh(M\eta) + C_{45}\cosh(M\eta) + C_{46}\sin(\sqrt{\phi}\eta) + C_{47}\cos(\sqrt{\phi}\eta) + \frac{48}{M^2}, \quad (63)$$

$$\theta = \frac{(\phi + M^2)}{Gr/Re}[C_{46}\sin(\sqrt{\phi}\eta) + C_{47}\cos(\sqrt{\phi}\eta)], \quad (64)$$

where

$$C_{44} = -C_{46}\frac{\sin(\sqrt{\phi}/4)}{\sinh(M/4)},$$
$$C_{45} = \frac{-48/M^2 - C_{47}\cos(\sqrt{\phi}/4)}{\cosh(M/4)},$$
$$C_{46} = \frac{-Gr/Re[\cos(\sqrt{\phi}/4) - R_{tq}\sqrt{\phi}\sin(\sqrt{\phi}/4)]}{\sqrt{\phi}(M^2+\phi)\cos(\sqrt{\phi}/2)}, \quad (65)$$
$$C_{47} = \frac{-Gr/Re[\sin(\sqrt{\phi}/4) - R_{tq}\sqrt{\phi}\cos(\sqrt{\phi}/4)]}{\sqrt{\phi}(M^2+\phi)\cos(\sqrt{\phi}/2)}$$

for the heat generation case and

$$U = C_{48}\sinh(M\eta) + C_{49}\cosh(M\eta) + C_{50}\sinh(\sqrt{\phi}\eta) + C_{51}\cosh(\sqrt{\phi}\eta) + \frac{48}{M^2}, \quad (66)$$

$$\theta = \frac{-(\phi - M^2)}{Gr/Re}[C_{50}\sinh(\sqrt{\phi}\eta) + C_{51}\cosh(\sqrt{\phi}\eta)], \quad (67)$$

$$C_{48} = -C_{50}\frac{\sinh(\sqrt{\phi}/4)}{\sinh(M/4)},$$
$$C_{49} = \frac{-48/M^2 - C_{51}\cosh(\sqrt{\phi}/4)}{\cosh(M/4)},$$
$$C_{50} = \frac{Gr/Re[\cosh(\sqrt{\phi}/4) + R_{tq}\sqrt{\phi}\sinh(\sqrt{\phi}/4)]}{\sqrt{\phi}(\phi - M^2)\cosh(\sqrt{\phi}/2)}, \quad (68)$$
$$C_{51} = \frac{Gr/Re[\sinh(\sqrt{\phi}/4) - R_{tq}\sqrt{\phi}\cosh(\sqrt{\phi}/4)]}{\sqrt{\phi}(\phi - M^2)\cosh(\sqrt{\phi}/2)}$$

for the heat absorption case.

4. Heat transfer aspects

The Nusselt numbers at each of the channel walls are important physical characteristics. These can be defined for the three different thermal boundary conditions considered in the present work as follows:

4.1. Isothermal–isothermal ($T_1 - T_2$) walls

$$Nu_1 = \frac{h_1 D}{k} = \frac{D}{\Delta T}\left.\frac{dT}{dy}\right|_{-L/2} = \theta'(-1/4),$$
$$Nu_2 = \frac{h_2 D}{k} = \frac{D}{\Delta T}\left.\frac{dT}{dy}\right|_{L/2} = \theta'(1/4), \quad (69)$$

where a prime denotes differentiation with respect to η and Nu_1 and Nu_2 are the Nusselt numbers at the left and right walls, respectively. h_1 and h_2 are the heat transfer coefficient evaluated at the left and right walls, respectively.

Application of Eqs. (69) for case 3 gives

$$Nu_1 = Nu_2 = \frac{R_t\sqrt{\phi}}{2}\cot(\sqrt{\phi}/4) \quad (70)$$

for the heat generation case and

$$Nu_1 = Nu_2 = \frac{R_t\sqrt{\phi}}{2}\coth(\sqrt{\phi}/4) \quad (71)$$

for the heat absorption case.

It can easily be shown by using the fact that the limit of $x\cot(x)$ or $(x\coth(x))$ as $x \to 0$ is equal to unity that in the absence of heat generation or absorption, the limits of Eqs. (70) and (71) as $\phi \to 0$ yield

$$Nu_1 = Nu_2 = 2R_t, \quad (72)$$

which is consistent with the result reported by Barletta [5].

4.2. Isoflux–isothermal ($q_1 - T_2$) walls

$$Nu_1 = \frac{h_1 D}{k} = \frac{Dq_1}{k(T_1 - T_0)} = \frac{1}{\theta_1},$$
$$Nu_2 = \frac{h_2 D}{k} = \frac{D}{\Delta T}\left(\frac{\mathrm{d}T}{\mathrm{d}y}\right)_2 = \theta_2', \tag{73}$$

where the quantities with subscripts 1 and 2 are understood to be evaluated at the left ($\eta = -1/4$) and right ($\eta = 1/4$) walls, respectively.

For the general case 6, Nu_1 and Nu_2 are given by

$$Nu_1 = \frac{Gr/Re}{(\phi + M^2)[C_{27}\cos(\sqrt{\phi}/4) - C_{26}\sin(\sqrt{\phi}/4)]}, \tag{74}$$

$$Nu_2 = \frac{\sqrt{\phi}(\phi + M^2)}{Gr/Re}[C_{26}\cos(\sqrt{\phi}/4) - C_{27}\sin(\sqrt{\phi}/4)] \tag{75}$$

for the heat generation case and

$$Nu_1 = -\frac{Gr/Re}{(\phi - M^2)[-C_{30}\sinh(\sqrt{\phi}/4) + C_{31}\cosh(\sqrt{\phi}/4)]}, \tag{76}$$

$$Nu_2 = \frac{-\sqrt{\phi}(\phi - M^2)}{Gr/Re}[C_{30}\cosh(\sqrt{\phi}/4) + C_{31}\sinh(\sqrt{\phi}/4)] \tag{77}$$

for the heat absorption case.

4.3. Isothermal–isoflux ($T_1 - q_2$) walls

$$Nu_1 = \frac{h_1 D}{k} = \frac{D}{\Delta T}\left(\frac{\mathrm{d}T}{\mathrm{d}y}\right)_1 = \theta_1',$$
$$Nu_2 = \frac{h_2 D}{k} = \frac{Dq_2}{k(T_2 - T_0)} = \frac{1}{\theta_2}. \tag{78}$$

Employing Eqs. (78) for the general case 9 yields the following Nusselt numbers:

$$Nu_1 = \frac{\sqrt{\phi}(\phi + M^2)}{Gr/Re}[C_{46}\cos(\sqrt{\phi}/4) + C_{47}\sin(\sqrt{\phi}/4)], \tag{79}$$

$$Nu_2 = \frac{Gr/Re}{(\phi + M^2)[C_{46}\sin(\sqrt{\phi}/4) + C_{47}\cos(\sqrt{\phi}/4)]} \tag{80}$$

for the heat generation case and

$$Nu_1 = -\frac{\sqrt{\phi}(\phi - M^2)}{Gr/Re}[C_{50}\cosh(\sqrt{\phi}/4) - C_{51}\sinh(\sqrt{\phi}/4)], \tag{81}$$

$$Nu_2 = -\frac{Gr/Re}{(\phi - M^2)[C_{50}\sinh(\sqrt{\phi}/4) + C_{51}\cosh(\sqrt{\phi}/4)]} \tag{82}$$

for the heat absorption case.

5. Reversed flow conditions

Depending on the value of the mixed convection parameter Gr/Re and the wall thermal boundary conditions, a flow reversal condition may occur. It is beneficial to understand when this situation occurs and determine a reversed flow zone associated with each of the problems discussed earlier. The occurrence of a reversed flow condition is ensured when the slopes of the velocity profile at the walls have the same sign. That is

$$[U'(-1/4)][U'(1/4)] > 0. \tag{83}$$

The critical condition for flow reversal at the walls occurs when the wall slopes vanish such that

$$U'(-1/4) = 0, \quad U'(1/4) = 0. \tag{84}$$

Therefore, the two lines given by Eqs. (84) constitute the borders of the reversed flow region.

The conditions for reversed flow are found below for the three general cases 3, 6 and 9. The other problems discussed earlier represent special cases of these three general ones.

5.1. Case 3

For this case, the velocity profile, is given by Eq. (24) for the heat generation case and by Eq. (26) for the heat absorption case. Differentiating U with respect to η, evaluating the result at both $\eta = -1/4$ and $\eta = 1/4$, and then solving for the mixed convection parameter Gr/Re produce the borders of the reversed flow regions. These can be shown to be

$$\left(\frac{Gr}{Re}\right)_1 = \frac{C_8 M \sinh(M/4)}{MC_7^* \cosh(M/4) + \sqrt{\phi}C_9^* \cos(\sqrt{\phi}/4)}, \tag{85}$$

$$\left(\frac{Gr}{Re}\right)_2 = -\left(\frac{Gr}{Re}\right)_1, \tag{86}$$

where the subscripts 1 and 2 correspond to the left ($\eta = -1/4$) and right ($\eta = 1/4$) walls, respectively, for the heat generation, case and

$$\left(\frac{Gr}{Re}\right)_1 = \frac{C_8 M \sinh(M/4)}{MC_{10}^* \cosh(M/4) + \sqrt{\phi}C_{11}^* \cosh(\sqrt{\phi}/4)}, \tag{87}$$

$$\left(\frac{Gr}{Re}\right)_2 = -\left(\frac{Gr}{Re}\right)_1 \tag{88}$$

for the heat absorption case. In Eqs. (85)–(88), the constants C_7^*, C_9^*, C_{10}^* and C_{11}^* are given by

$$\begin{aligned} C_7^* &= -\frac{R_t}{2(M^2+\phi)\sinh(M/4)}, \\ C_9^* &= \frac{R_t}{2(M^2+\phi)\sin(\sqrt{\phi}/4)}, \\ C_{10}^* &= -\frac{R_t}{2(M^2-\phi)\sinh(M/4)}, \\ C_{11}^* &= \frac{R_t}{2(M^2-\phi)\sinh(\sqrt{\phi}/4)}. \end{aligned} \tag{89}$$

It should be noted that, with some involved mathematical manipulation, the limits of Eqs. (85)–(88) as both of M and ϕ approach zero can be shown to lead to $(Gr/Re)_2 = -(Gr/Re)_1 = -288/R_t$. Then, for $R_t = 1$ (asymmetric heating) $(Gr/Re)_2 = -(Gr/Re)_1 = -288$ which is the same result reported by Barletta [5].

5.2. Case 6

The reversed flow conditions for this case are obtained by the same way as done for case 3. Without going into details the mixed convection parameter for these conditions can be shown to be

$$\begin{aligned} \left(\frac{Gr}{Re}\right)_1 &= -48/M\tanh(M/4)/[C_{24}^* M\cosh(M/4) \\ &\quad + C_{27}^* M\tanh(M/4)\cos(\sqrt{\phi}/4) \\ &\quad + C_{26}^*\sqrt{\phi}\cos(\sqrt{\phi}/4) \\ &\quad + C_{27}^*\sqrt{\phi}\sin(\sqrt{\phi}/4)], \end{aligned} \tag{90}$$

$$\begin{aligned} \left(\frac{Gr}{Re}\right)_2 &= 48/M\tanh(M/4)/[C_{24}^* M\cosh(M/4) \\ &\quad - C_{27}^* M\tanh(M/4)\cos(\sqrt{\phi}/4) \\ &\quad + C_{26}^*\sqrt{\phi}\cos(\sqrt{\phi}/4) \\ &\quad - C_{27}^*\sqrt{\phi}\sin(\sqrt{\phi}/4)], \end{aligned} \tag{91}$$

where

$$\begin{aligned} C_{24}^* &= \frac{-C_{26}^*\sin(\sqrt{\phi}/4)}{\sinh(M/4)}, \\ C_{26}^* &= \frac{-R_{qt}\sqrt{\phi}\sin(\sqrt{\phi}/4)-\cos(\sqrt{\phi}/4)}{\sqrt{\phi}(M^2+\phi)\cos(\sqrt{\phi}/2)}, \\ C_{27}^* &= \frac{R_{qt}\sqrt{\phi}\cos(\sqrt{\phi}/4)+\sin(\sqrt{\phi}/4)}{\sqrt{\phi}(M^2+\phi)\cos(\sqrt{\phi}/2)} \end{aligned} \tag{92}$$

for the heat generation case and

$$\begin{aligned} \left(\frac{Gr}{Re}\right)_1 &= -48/M\tanh(M/4)/[C_{28}^* M\cosh(M/4) \\ &\quad + C_{31}^* M\tanh(M/4)\cosh(\sqrt{\phi}/4) \\ &\quad + C_{30}^*\sqrt{\phi}\cosh(\sqrt{\phi}/4) \\ &\quad - C_{31}^*\sqrt{\phi}\sinh(\sqrt{\phi}/4)], \end{aligned} \tag{93}$$

$$\begin{aligned} \left(\frac{Gr}{Re}\right)_2 &= 48/M\tanh(M/4)/[C_{28}^* M\cosh(M/4) \\ &\quad - C_{31}^* M\tanh(M/4)\cosh(\sqrt{\phi}/4) \\ &\quad + C_{30}^*\sqrt{\phi}\cosh(\sqrt{\phi}/4) \\ &\quad + C_{31}^*\sqrt{\phi}\sinh(\sqrt{\phi}/4)], \end{aligned} \tag{94}$$

where

$$\begin{aligned} C_{28}^* &= \frac{-C_{30}^*\sin(\sqrt{\phi}/4)}{\sinh(M/4)}, \\ C_{30}^* &= \frac{\cosh(\sqrt{\phi}/4)-R_{qt}\sqrt{\phi}\sinh(\sqrt{\phi}/4)}{\sqrt{\phi}(\phi-M^2)\cosh(\sqrt{\phi}/2)}, \\ C_{31}^* &= \frac{-\sinh(\sqrt{\phi}/4)-R_{qt}\sqrt{\phi}\cosh(\sqrt{\phi}/4)}{\sqrt{\phi}(\phi-M^2)\cosh(\sqrt{\phi}/2)} \end{aligned} \tag{95}$$

for the heat absorption case.

5.3. Case 9

The expressions for the mixed convection parameter for which reversed flow conditions near the walls exist can be shown for this case to be

$$\begin{aligned} \left(\frac{Gr}{Re}\right)_1 &= -48/M\tanh(M/4)\Big/\Big[C_{44}^* M\cosh(M/4) \\ &\quad + C_{47}^* M\tanh(M/4)\cos(\sqrt{\phi}/4) \\ &\quad + C_{46}^*\sqrt{\phi}\cos(\sqrt{\phi}/4) \\ &\quad + C_{47}^*\sqrt{\phi}\sin(\sqrt{\phi}/4)\Big], \end{aligned} \tag{96}$$

$$\begin{aligned} \left(\frac{Gr}{Re}\right)_2 &= 48/M\tanh(M/4)\Big/\Big[C_{44}^* M\cosh(M/4) \\ &\quad - C_{47}^* M\tanh(M/4)\cos(\sqrt{\phi}/4) \\ &\quad + C_{46}^*\sqrt{\phi}\cos(\sqrt{\phi}/4) \\ &\quad - C_{47}^*\sqrt{\phi}\sin(\sqrt{\phi}/4)\Big], \end{aligned} \tag{97}$$

where

$$\begin{aligned} C_{44}^* &= -C_{46}^*\frac{\sin(\sqrt{\phi}/4)}{\sinh(M/4)}, \\ C_{46}^* &= \frac{-[\cos(\sqrt{\phi}/4)-R_{tq}\sqrt{\phi}\sin(\sqrt{\phi}/4)]}{\sqrt{\phi}(M^2+\phi)\cos(\sqrt{\phi}/2)}, \\ C_{47}^* &= \frac{-[\sin(\sqrt{\phi}/4)-R_{tq}\sqrt{\phi}\cos(\sqrt{\phi}/4)]}{\sqrt{\phi}(M^2+\phi)\cos(\sqrt{\phi}/2)} \end{aligned} \tag{98}$$

for the heat generation case and

$$\begin{aligned} \left(\frac{Gr}{Re}\right)_1 &= -48/M\tanh(M/4)\Big/\Big[C_{48}^* M\cosh(M/4) \\ &\quad + C_{51}^* M\tanh(M/4)\cosh(\sqrt{\phi}/4) \\ &\quad + C_{50}^*\sqrt{\phi}\cosh(\sqrt{\phi}/4) \\ &\quad - C_{51}^*\sqrt{\phi}\sinh(\sqrt{\phi}/4)\Big], \end{aligned} \tag{99}$$

$$\left(\frac{Gr}{Re}\right)_2 = 48/M\tanh(M/4)\Big/\Big[C^*_{48}M\cosh(M/4) - C^*_{51}M\tanh(M/4)\cosh(\sqrt{\phi}/4) + C^*_{50}\sqrt{\phi}\cosh(\sqrt{\phi}/4) + C^*_{51}\sqrt{\phi}\sinh(\sqrt{\phi}/4)\Big], \quad (100)$$

where

$$C^*_{48} = -C^*_{50}\frac{\sinh(\sqrt{\phi}/4)}{\sinh(M/4)},$$
$$C^*_{50} = \frac{\cosh(\sqrt{\phi}/4) + R_{tq}\sqrt{\phi}\sinh(\sqrt{\phi}/4)}{\sqrt{\phi}(\phi - M^2)\cosh(\sqrt{\phi}/2)}, \quad (101)$$
$$C^*_{51} = \frac{\sinh(\sqrt{\phi}/4) - R_{tq}\sqrt{\phi}\cosh(\sqrt{\phi}/4)}{\sqrt{\phi}(\phi - M^2)\cosh(\sqrt{\phi}/2)}$$

for the heat absorption case.

6. Selected graphical results

Fig. 2 displays typical velocity profiles U in a vertical channel with asymmetric ($R_t = 1.0$) isothermal–isothermal wall heating conditions for different values of the mixed convection parameter Gr/Re. For a vanishing value of Gr/Re, the usual symmetric Hagen–Poiseuille velocity profile is obtained. For an upward flow, increases in the value of Gr/Re have the tendency to increase the momentum of the flow close to the hot right wall causing the velocity profile to become asymmetric. As mentioned before, it is expected that beyond a critical value of Gr/Re, a flow, reversal condition near the cold left wall occurs and that this phenomenon increases further as Gr/Re increases. Similarly, for a downward flow, the induced flow increases close to the cold wall with the reversed flow phenomenon occurring close to the hot wall. The values of $Gr/Re = 213$ and $Gr/Re = -213$ are obtained from Eqs. (85) and (86), respectively, and they represent the positive and negative critical values of Gr/Re. That is, for $Gr/Re > 213$ a reversed flow occurs close to the cold wall and for $Gr/Re < -213$ a reversed flow takes place near the hot wall. These behaviors are clearly depicted in Fig. 2.

Fig. 3 presents representative velocity profiles U in a vertical channel with asymmetric isothermal–isothermal wall conditions for various values of the Hartmann number M and two chosen values of the mixed convection parameters Gr/Re. The chosen values of $Gr/Re = 288$ and $Gr/Re = -288$ represent the critical conditions for flow reversal at the left and right walls, respectively, in the absence of the magnetic and heat generation or absorption effects. That is, any value of $Gr/Re > 288$ results in reversed flow near the left wall and any value of $Gr/Re < -288$ produces flow reversal at the right wall. This figure serves dual purposes. It

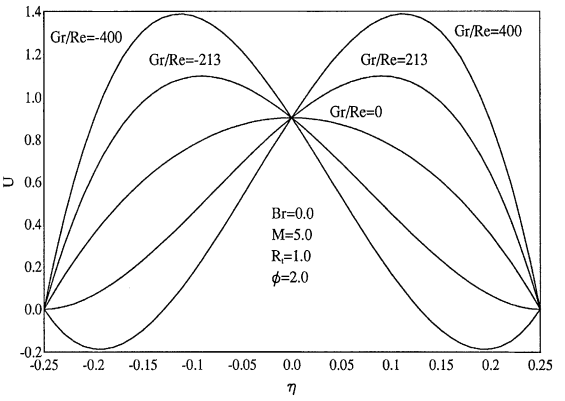

Fig. 2. Effects of Gr/Re on velocity profiles for $(T_1 - T_2)$ case.

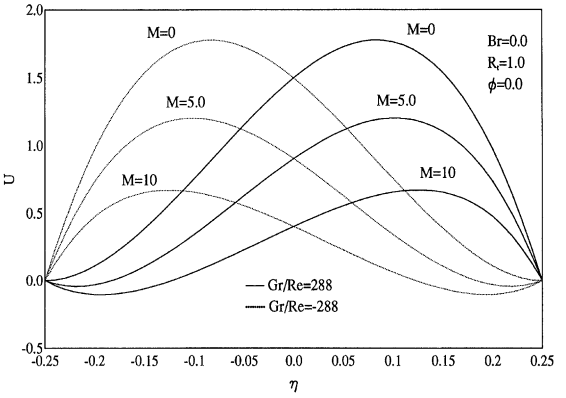

Fig. 3. Effects of M on velocity profiles for $(T_1 - T_2)$ case.

shows the effect of the magnetic field on the fluid flow in the channel and its influence on the flow reversal conditions. Application of a transverse magnetic field to an electrically conducting fluid gives rise to the magnetic Lorentz force which acts in the direction opposite to that of the fluid causing it to slow down. This drag-like force increases as the strength of the magnetic field (represented by Hartmann number M) increases producing further reductions in the fluid velocity. For the buoyancy aiding flow case where $Gr/Re = 288$, increasing the Hartmann number reduces the fluid adjacent to the cold left wall causing a flow reversal condition there. This reversed flow phenomenon increases as the strength of the magnetic field increases. For the buoyancy opposing flow case where $Gr/Re = -288$, the same phenomenon of reversed flow occurs but close to the hot right wall.

Figs. 4 and 5 illustrate the influence of both the Hartmann number M and the heat generation or absorption coefficient ϕ on the velocity profiles in a vertical channel with isoflux–isothermal wall conditions, respectively, In each of these figures, two conditions of thermal buoyancy and thermal ratio parameters ($R_{qt} = -0.5, 0.5$) are considered. For a given value of R_{qt}, the corresponding

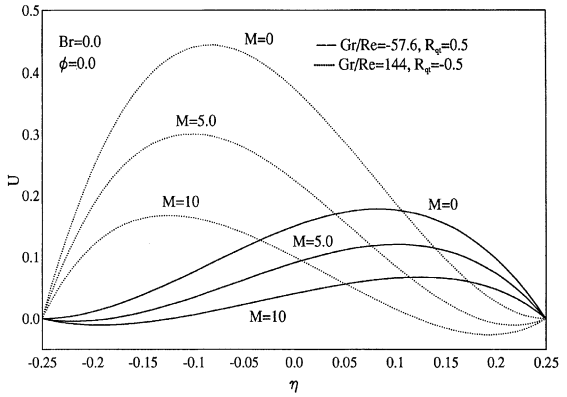

Fig. 4. Effects of M on velocity profiles for $(q_1 - T_2)$ case.

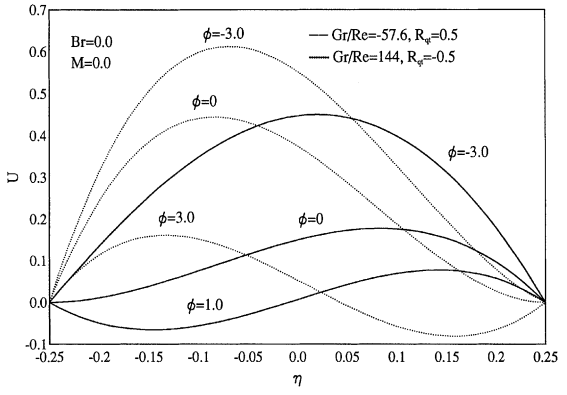

Fig. 5. Effects of ϕ on velocity profiles for $(q_1 - T_2)$ case.

critical values of Gr/Re are obtained from the analytical solutions for reversed flow conditions associated with the isoflux–isothermal wall conditions reported in Eqs. (90)–(95). Similar to Fig. 3, Fig. 4 shows that the effect of increasing the value of M produces reduced flow in the channel and reversed flow near the left wall with constant heat flux for $R_{qt} = 0.5$ and close to the isothermal right wall for $R_{qt} = -0.5$. In Fig. 5, it is seen that heat generation ($\phi > 0$) reduces the flow in the channel while heat absorption, ($\phi < 0$) increases the fluid velocity in the channel for the two considered values of the thermal ratio parameter R_{qt}. In addition, it is predicted that a reversed flow condition occurs close to the left wall for $Gr/Re = -57.6$ and $R_{qt} = 0.5$ with heat generation ($\phi = 1.0$) and close to the right wall for $Ge/Re = 144$ and $R_{qt} = -0.5$ with $\phi = 3.0$. The region of reversed flow increases as the value of ϕ increases for both cases.

Fig. 6 displays the influence of ϕ on the temperature profiles in a vertical channel with isoflux–isothermal walls for both $R_{qt} = 0.5$ and $R_{qt} = -0.5$. It is seen that the temperature at the wall with constant heat flux decreases as the heat generation or absorption coefficient ϕ increases for both values of R_{qt} considered. However, the

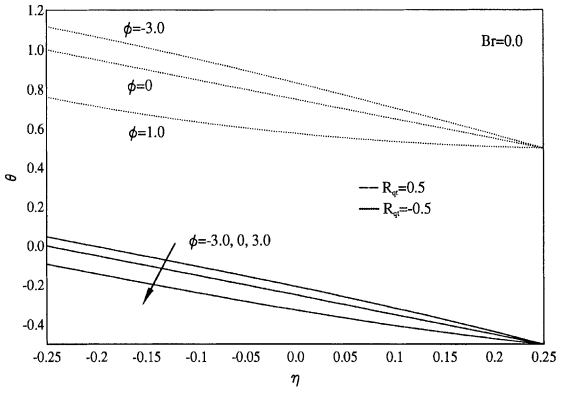

Fig. 6. Effects of ϕ on temperature profiles for $(q_1 - T_2)$ case.

wall temperature is more influenced for the case of $R_{qt} = -0.5$ than for the case of $R_{qt} = 0.5$.

Fig. 7 depicts the variations in the velocity profiles U in a vertical channel with isothermal–isoflux wall conditions as a result of changing M or ϕ for a thermal ratio parameter $R_{qt} = 0.5$ and a mixed convection parameter $Gr/Re = -144$. This figure predicts the same behaviors as those observed in Figs. 4 and 5 for the isoflux–isothermal case. That is, owing the presence of either of the magnetic field or the heat generation effects, the fluid velocity in the channel decreases and reversed flow occurs close to the isothermal walls.

In Fig. 8, the value of Gr/Re required for flow reversal close to the cold left wall for the isothermal–isothermal walls case as a function of R_t for different values of M and ϕ is plotted. For $R_t = 0$ (symmetric isothermal wall heating) no reversed flow occurs. However, $R_t \neq 0$, the velocity profiles in the channel become asymmetric and flow reversal close to the cold wall may occur. The degree of asymmetry increases as R_t increases and the flow reversal critical value of Gr/Re decreases inversely with R_t as shown previously. Again, the effects of the magnetic field and heat generation produce reversed flow near the

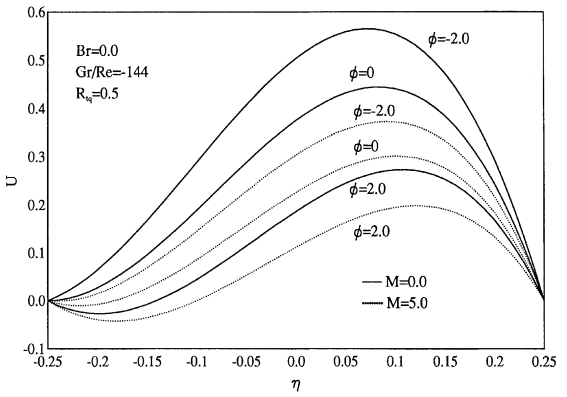

Fig. 7. Effects of M and ϕ on velocity profiles for $(T_1 - q_2)$ case.

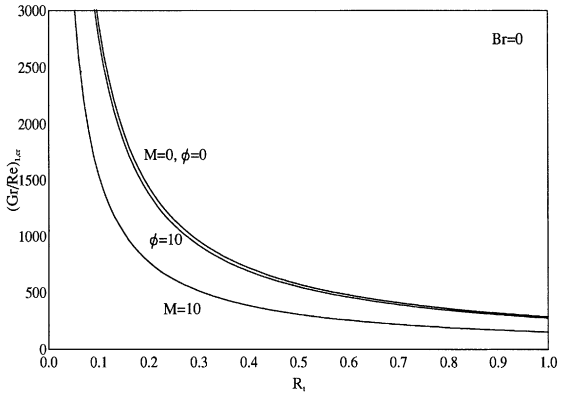

Fig. 8. Effects of M and ϕ on reversed flow for $(T_1 - T_2)$ case.

cold wall in the neighborhood of the critical value of Gr/Re. Therefore, the critical value of Gr/Re decreases as either M or ϕ increases for all values of R_t. These behaviors are apparent from Fig. 8. It is also noted that the influence of M on the critical value of Gr/Re is stronger than that of ϕ especially for the isothermal walls case. As predicted by Eq. (86), the critical value of Gr/Re for reversed flow close to the hot right wall is exactly the negative of the critical value of Gr/Re associated with the cold wall for all values of M, R_t, and ϕ.

The effects of the heat generation or absorption, coefficient ϕ and the thermal ratio parameters (R_t, R_{qt} and R_{tq}) on the Nusselt number for the isothermal–isothermal, isoflux–isothermal and the isothermal–isoflux cases are presented in Figs. 9 through 11, respectively. For the isothermal–isothermal case, it is predicted that the Nusselt number at the cold wall (or the hot wall as predicted by Eqs. (70) and (71)) increases with increases in the values of R_t and decreases as the value of ϕ increases as shown in Fig. 9. However, for the isoflux–isothermal and isothermal–isoflux cases, the Nusselt numbers at the isothermal walls are uniform for the case of $\phi = 0$ for all values of R_{qt} and R_{tq} while they decrease or increase with

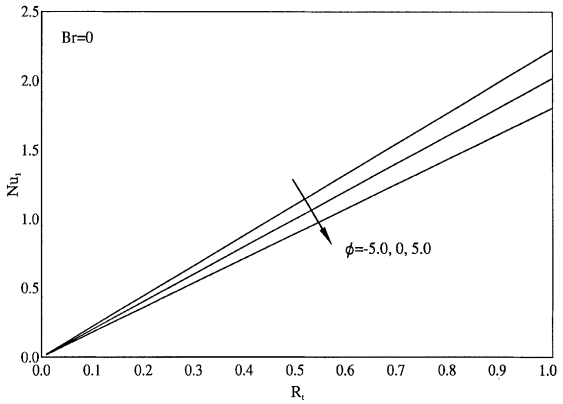

Fig. 9. Effects of R_t and ϕ on Nusselt number.

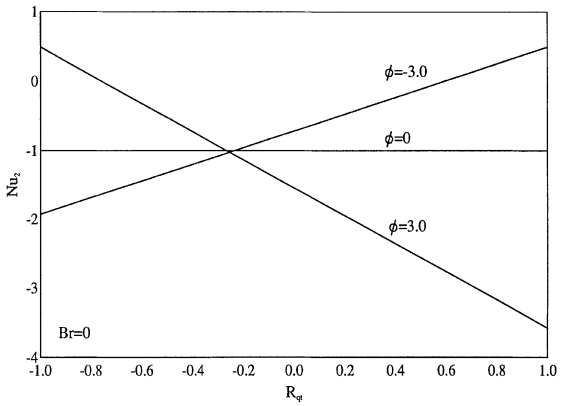

Fig. 10. Effects of R_{qt} and ϕ on Nusselt number.

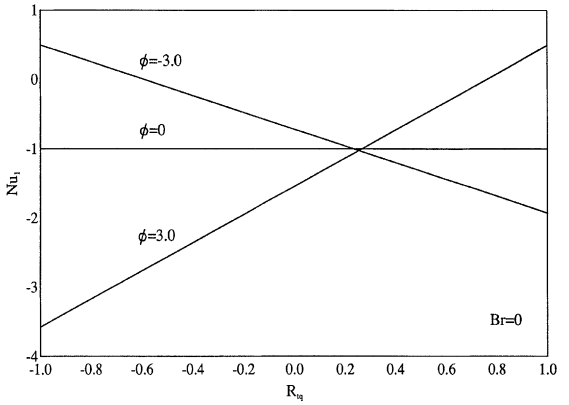

Fig. 11. Effects of R_{tq} and ϕ on Nusselt number.

R_{qt} and R_{tq} depending on the value of $\phi \neq 0$. For example, the Nusselt number at the right wall (Nu_2) for the isoflux–isothermal case decreases with R_{qt} for heat generation ($\phi > 0$) while it increases with R_{qt} when heat absorption effects ($\phi < 0$) are present. The opposite effect is predicted for the Nusselt number at the left wall (Nu_1) for the isothermal–isoflux case for which (Nu_1) increases with R_{tq} for $\phi > 0$ and decreases with R_{tq} for $\phi < 0$. In addition, the values of Nu_2 (for the case of isoflux–isothermal case) and Nu_1 (for the case of isothermal–isoflux case) are the same at the intersection, points when $R_{qt} = -0.25$ and $R_{tq} = 0.25$ for all values of $\phi \neq 0$. It is observed that the influence of heat generation, ($\phi = 3.0$) on both, Nu_2 and Nu_1 for both cases is more pronounced than that of the corresponding heat absorption value $\phi = 3.0$. These facts are apparent from Figs. 10 and 11.

6.1. Analytical solutions for forced convection in a channel with viscous dissipation and Joule heating

In this section, closed-form solutions for the velocity and temperature profiles as well as the Nusselt numbers

are obtained when both viscous dissipation and Joule heating are present and buoyancy effects are absent. For this situation the following equations and boundary conditions hold:

$$U'' - M^2U + 48 = 0, \tag{102}$$

$$\theta'' + \phi\theta + Br(U')^2 + BrM^2U^2 = 0, \tag{103}$$

$$U(-1/4) = U(1/4) = 0, \tag{104}$$

$$\theta(-1/4) = -R_t/2,$$
$$\theta(1/4) = R_t/2 \quad \text{for } (T_1 - T_2) \text{ case}, \tag{105}$$

$$\theta'(-1/4) = -1,$$
$$\theta(1/4) = R_{qt} \quad \text{for } (q_1 - T_2) \text{ case}, \tag{106}$$

$$\theta(-1/4) = -R_{tq},$$
$$\theta'(1/4) = -1 \quad \text{for } (T_1 - q_2) \text{ case}. \tag{107}$$

Without going into detail, it can be shown that the solutions for U and θ for the case of heat generation ($\phi > 0$) can be written as

$$U = (48/M^2)[1 - \operatorname{sech}(M/4)\cosh(M\eta)], \tag{108}$$

$$\theta = N_1 + N_2\cosh(2M\eta) + N_3\cosh(M\eta) + N_4\cos(\sqrt{\theta}\eta) + N_5\sin(\sqrt{\phi}\eta), \tag{109}$$

where

$$N_1 = -\frac{Br(48/M^2)^2}{\phi},$$
$$N_2 = -\frac{Br(48/M^2)^2\operatorname{sech}^2(M/4)}{4M^2 + \phi}, \tag{110}$$
$$N_3 = \frac{2Br(48/M^2)^2\operatorname{sech}(M/4)}{M^2 + \phi}$$

and

$$N_4 = -\frac{[N_1 + N_2\cosh(M/2) + N_3\cosh(M/4)]}{\cos(\sqrt{\phi}/4)},$$
$$N_5 = \frac{R_t}{2\sin(\sqrt{\phi}/4)} \tag{111}$$

for the isothermal–isothermal $(T_1 - T_2)$ case;

$$\begin{aligned} N_4 = \Big\{ & R_{qt}\sqrt{\phi}\cos(\sqrt{\phi}/4) + \sin(\sqrt{\phi}/4) \\ & - N_2\Big[\sqrt{\phi}\cos(\sqrt{\phi}/4)\cosh(M/2) \\ & + 2M\sin(\sqrt{\phi}/4)\sinh(M/2)\Big] \\ & - N_3\Big[\sqrt{\phi}\cos(\sqrt{\phi}/4)\cosh(M/4) \\ & + M\sin(\sqrt{\phi}/4)\sinh(M/4)\Big] \\ & - N_1\sqrt{\phi}\cos(\sqrt{\phi}/4)\Big\}\Big/\Big[\sqrt{\phi}\cos(\sqrt{\phi}/2)\Big], \end{aligned}$$

$$\begin{aligned} N_5 = \Big\{ & R_{qt}\sqrt{\phi}\sin(\sqrt{\phi}/4) + \cos(\sqrt{\phi}/4) \\ & - N_2\Big[2M\sinh(M/2)\cos(\sqrt{\phi}/4) \\ & + \sqrt{\phi}\sin(\sqrt{\phi}/4)\cosh(M/2)\Big] \\ & - N_3\Big[M\sinh(M/4)\cos(\sqrt{\phi}/4) \\ & + \sqrt{\phi}\sin(\sqrt{\phi}/4)\cosh(M/4)\Big] \\ & - N_1\sqrt{\phi}\sin(\sqrt{\phi}/4)\Big\}\Big/\Big[-\sqrt{\phi}\cos(\sqrt{\phi}/2)\Big] \end{aligned} \tag{112}$$

for the isoflux–isothermal $(q_1 - T_2)$ case;

$$\begin{aligned} N_4 = \Big\{ & R_{tq}\sqrt{\phi}\cos(\sqrt{\phi}/4) - \sin(\sqrt{\phi}/4) \\ & - N_2\Big[2M\sinh(M/2)\sin(\sqrt{\phi}/4) \\ & + \sqrt{\phi}\cos(\sqrt{\phi}/4)\cosh(M/2)\Big] \\ & - N_3\Big[M\sinh(M/4)\sin(\sqrt{\phi}/4) \\ & + \sqrt{\phi}\cos(\sqrt{\phi}/4)\cosh(M/4)\Big] \\ & - N_1\sqrt{\phi}\cos(\sqrt{\phi}/4)\Big\}\Big/\Big[\sqrt{\phi}\cos(\sqrt{\phi}/2)\Big], \end{aligned}$$

$$\begin{aligned} N_5 = \Big\{ & R_{tq}\sqrt{\phi}\sin(\sqrt{\phi}/4) - \cos(\sqrt{\phi}/4) \\ & - N_2\Big[2M\sinh(M/2)\cos(\sqrt{\phi}/4) \\ & + \sqrt{\phi}\sin(\sqrt{\phi}/4)\cosh(M/2)\Big] \\ & - N_3\Big[M\sinh(M/4)\cos(\sqrt{\phi}/4) \\ & + \sqrt{\phi}\sin(\sqrt{\phi}/4)\cosh(M/4)\Big] \\ & - N_1\sqrt{\phi}\cos(\sqrt{\phi}/4)\Big\}\Big/\Big[\sqrt{\phi}\cos(\sqrt{\phi}/2)\Big] \end{aligned} \tag{113}$$

for the isothermal–isoflux $(T_1 - q_2)$ case.

The corresponding temperature distribution solutions for fthe case of heat absorption are obtained by replacing ϕ in Eq. (103) by $-\phi$ and solving subject Eqs. (105)–(107). These solutions can be written as

$$\theta = N_1^* + N_2^*\cosh(2M\eta) + N_3^*\cosh(M\eta) + N_4^*\cosh(\sqrt{\phi}\eta) + N_5^*\sinh(\sqrt{\phi}/4), \tag{114}$$

where

$$N_1^* = -N_1, \quad N_2 = -\frac{Br(48/M^2)^2\operatorname{sech}^2(M/4)}{4M^2 - \phi},$$
$$N_3^* = \frac{2Br(48/M^2)^2\operatorname{sech}(M/4)}{M^2 - \phi} \tag{115}$$

and

$$N_4^* = -\frac{[N_1^* + N_2^*\cosh(M/2) + N_3^*\cosh(M/4)]}{\cosh(\sqrt{\phi}/4)},$$
$$N_5^* = \frac{R_t}{2\sinh(\sqrt{\phi}/4)} \tag{116}$$

for the isothermal–isothermal $(T_1 - T_2)$ case

$$\begin{aligned}N_4^* = {} & \Big\{R_{qt}\sqrt{\phi}\cosh(\sqrt{\phi}/4) + \sinh(\sqrt{\phi}/4) \\ & - N_2^*\Big[\sqrt{\phi}\cosh(\sqrt{\phi}/4)\cosh(M/2) \\ & + 2M\sinh(M/2)\sinh(\sqrt{\phi}/4)\Big] \\ & - N_3^*\Big[\sqrt{\phi}\cosh(\sqrt{\phi}/4)\cosh(M/4) \\ & + M\sinh(M/4)\sinh(\sqrt{\phi}/4)\Big] \\ & - N_1^*\sqrt{\phi}\cosh(\sqrt{\phi}/4)\Big\}\Big/\Big[\sqrt{\phi}\cosh(\sqrt{\phi}/2)\Big], \\ N_5^* = {} & \Big\{R_{qt}\sqrt{\phi}\sinh(\sqrt{\phi}/4) - \cosh(\sqrt{\phi}/4) \\ & - N_2^*\Big[\sqrt{\phi}\sinh(\sqrt{\phi}/4)\cosh(M/2) \\ & - 2M\sinh(M/2)\cosh(\sqrt{\phi}/4)\Big] \\ & - N_3^*\Big[\sqrt{\phi}\sinh(\sqrt{\phi}/4)\cosh(M/4) \\ & - M\sinh(M/4)\cosh(\sqrt{\phi}/4)\Big] \\ & - N_1^*\sqrt{\phi}\sinh(\sqrt{\phi}/4)\Big\}\Big/\Big[\sqrt{\phi}\cosh(\sqrt{\phi}/2)\Big]\end{aligned} \tag{117}$$

for the isoflux–isothermal $(q_1 - T_2)$ case

$$\begin{aligned}N_4^* = {} & \Big\{R_{tq}\sqrt{\phi}\cosh(\sqrt{\phi}/4) - \sinh(\sqrt{\phi}/4) \\ & - N_2^*\Big[\sqrt{\phi}\cosh(\sqrt{\phi}/4)\cosh(M/2) \\ & + 2M\sinh(M/2)\sinh(\sqrt{\phi}/4)\Big] \\ & - N_3^*\Big[\sqrt{\phi}\cosh(\sqrt{\phi}/4)\cosh(M/4) \\ & + M\sinh(M/4)\sinh(\sqrt{\phi}/4)\Big] \\ & - N_1^*\sqrt{\phi}\cosh(\sqrt{\phi}/4)\Big\}\Big/\Big[\sqrt{\phi}\cosh(\sqrt{\phi}/2)\Big], \\ N_5^* = {} & \Big\{ - R_{tq}\sqrt{\phi}\sinh(\sqrt{\phi}/4) - \cosh(\sqrt{\phi}/4) \\ & - N_2^*\Big[- \sqrt{\phi}\sinh(\sqrt{\phi}/4)\cosh(M/2) \\ & + 2M\sinh(M/2)\cosh(\sqrt{\phi}/4)\Big] \\ & - N_3^*\Big[- \sqrt{\phi}\sinh(\sqrt{\phi}/4)\cosh(M/4) \\ & + M\sinh(M/4)\cosh(\sqrt{\phi}/4)\Big] \\ & + N_1^*\sqrt{\phi}\sinh(\sqrt{\phi}/4)\Big\}\Big/\Big[\sqrt{\phi}\cosh(\sqrt{\phi}/2)\Big]\end{aligned} \tag{118}$$

for the isoflux–isothermal $(T_1 - q_2)$ case.

The Nusslet numbers for the above wall heating situations can be written as:

Isothermal–Isothermal $(T_1 - T_2)$ *Walls*:

$$\begin{aligned}Nu_1 = {} & -2MN_2\sinh(M/2) - MN_3\sinh(M/4) \\ & + N_4\sqrt{\phi}\sin(\sqrt{\phi}/4) + N_5\sqrt{\phi}\cos(\sqrt{\phi}/4), \\ Nu_2 = {} & 2MN_2\sinh(M/2) + MN_3\sinh(M/4) \\ & - N_4\sqrt{\phi}\sin(\sqrt{\phi}/4) + N_5\sqrt{\phi}\cos(\sqrt{\phi}/4).\end{aligned} \tag{119}$$

Isoflux–Isothermal $(q_1 - T_2)$ *walls*:

$$\begin{aligned}Nu_1 = {} & 1\Big/\Big[N_1 + N_2\cosh(M/2) + N_3\cosh(M/4) \\ & + N_4\cos(\sqrt{\phi}/4) - N_5\sin(\sqrt{\phi}/4)\Big], \\ Nu_2 = {} & 2MN_2\sinh(M/2) + MN_3\sinh(M/4) \\ & - N_4\sqrt{\phi}\sin(\sqrt{\phi}/4) + N_5\sqrt{\phi}\cos(\sqrt{\phi}/4).\end{aligned} \tag{120}$$

Isothermal–Isoflux $(T_1 - q_2)$ *walls*:

$$\begin{aligned}Nu_1 = {} & -2MN_2\sinh(M/2) - MN_3\sinh(M/4) \\ & + N_4\sqrt{\phi}\sin(\sqrt{\phi}/4) + N_5\sqrt{\phi}\cos(\sqrt{\phi}/4), \\ Nu_2 = {} & 1\Big/\Big[N_1 + N_2\cosh(M/2) + N_3\cosh(M/4) \\ & + N_4\cos(\sqrt{\phi}/4) + N_5\sin(\sqrt{\phi}/4)\Big]\end{aligned} \tag{121}$$

for the heat generation case and

Isothermal–Isothermal $(T_1 - T_2)$ *walls*:

$$\begin{aligned}Nu_1 = {} & -2MN_2^*\sinh(M/2) - MN_3^*\sinh(M/4) \\ & - N_4^*\sqrt{\phi}\sinh(\sqrt{\phi}/4) + N_5^*\sqrt{\phi}\cosh(\sqrt{\phi}/4), \\ Nu_2 = {} & 2MN_2^*\sinh(M/2) + MN_3^*\sinh(M/4) \\ & + N_4^*\sqrt{\phi}\sinh(\sqrt{\phi}/4) + N_5^*\sqrt{\phi}\cosh(\sqrt{\phi}/4).\end{aligned} \tag{122}$$

Isoflux–Isothermal $(q_1 - T_2)$ *walls*:

$$\begin{aligned}Nu_1 = {} & 1\Big/\Big[N_1^* + N_2^*\cosh(M/2) + N_3^*\cosh(M/4) \\ & + N_4^*\cosh(\sqrt{\phi}/4) - N_5^*\sinh(\sqrt{\phi}/4)\Big], \\ Nu_2 = {} & 2MN_2^*\sinh(M/2) + MN_3^*\sinh(M/4) \\ & + N_4^*\sqrt{\phi}\sinh(\sqrt{\phi}/4) + N_5^*\sqrt{\phi}\cosh(\sqrt{\phi}/4).\end{aligned} \tag{123}$$

Isothermal–Isoflux $(T_1 - q_2)$ *walls*:

$$\begin{aligned}Nu_1 = {} & -2MN_2^*\sinh(M/2) - MN_3^*\sinh(M/4) \\ & - N_4^*\sqrt{\phi}\sinh(\sqrt{\phi}/4) + N_5^*\sqrt{\phi}\cosh(\sqrt{\phi}/4), \\ Nu_2 = {} & 1\Big/\Big[N_1^* + N_2^*\cosh(M/2) + N_3^*\cosh(M/4) \\ & + N_4^*\cos(\sqrt{\phi}/4) + N_5^*\sin(\sqrt{\phi}/4)\Big]\end{aligned} \tag{124}$$

for the heat absorption case.

It can be shown (at least numerically) that as both M and ϕ approach zero, the solutions for θ given in Eqs. (109) and (114) and the Nusselt number solutions given in Eqs. (119) and (122) reduce to

$$\theta = -192Br\eta^4 + 2R_t\eta + \frac{3Br}{4}, \tag{125}$$

$$Nu_1 = 2(R_t + 6Br), \quad Nu_2 = 2(R_t - 6Br), \tag{126}$$

which are the same as reported by Cheng and Wu [8] and Barletta [5].

Fig. 12 illustrates the influence of the Brinkman number Br on the temperature profiles for the isothermal–isothermal case based on the analytical solutions given by Eq. (109) for $R_t = 0.5$ and $R_t = 1.0$. It is clearly seen that the linear temperature distribution associated with $Br = 0$ is no longer existing for the cases where $Br \neq 0$. In addition, the thermal state of the fluid is augmented owing the presence of both viscous and magnetic dissipations ($Br \neq 0$) for the two different asymmetic wall heat conditions ($R_t = 0.5$ and $R_t = 1.0$) shown.

In Fig. 13, the effect of Brinkman number Br on the temperature distribution in the channel for the case of isoflux–isothermal wall conditions is reported for two different values of the thermal ratio parameter R_{qt}. As in the case of isothermal– isothermal walls shown in Fig. 12, increasing the value of Br is seen to enhance the temperature distribution in the channel. However, in this case, the wall temperature of the left isoflux wall also increases. It is also seen that higher temperature distributions are obtained for higher values of R_{qt}.

Fig. 14 depicts the variations in the Nusselt number at the left and right walls of the channel as a result of changing Br for two different wall heating conditions. For the two shown cases, it is observed that while the Nusselt numbers at the left wall (Nu_1) increase with increasing values of Br, the Nusselt numbers at the right walls (Nu_2) show a decreasing trend with Br. It is interesting to note that while Nu_2 for the isothermal–isothermal case decreases linearly with Br, Nu_2 for the isothermal–isoflux case shows a nonlinear decay with Br approaching a constant value for large values of Br.

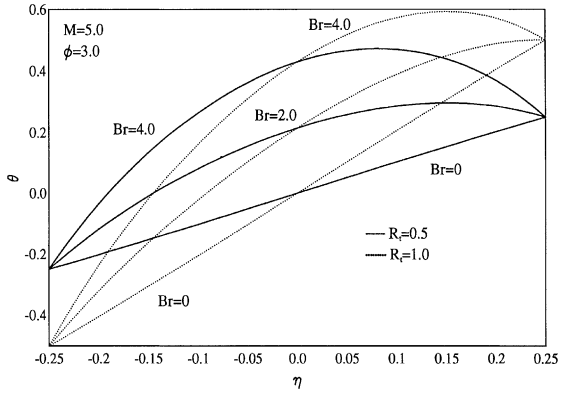

Fig. 12. Effects of Br on temperature profiles for $(T_1 - T_2)$ case.

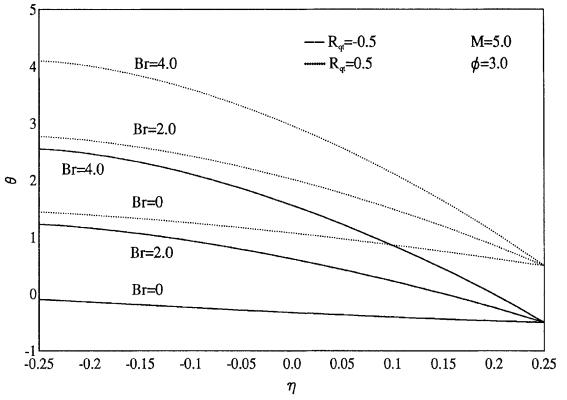

Fig. 13. Effects of Br on temperature profiles for $(q_1 - T_2)$ case.

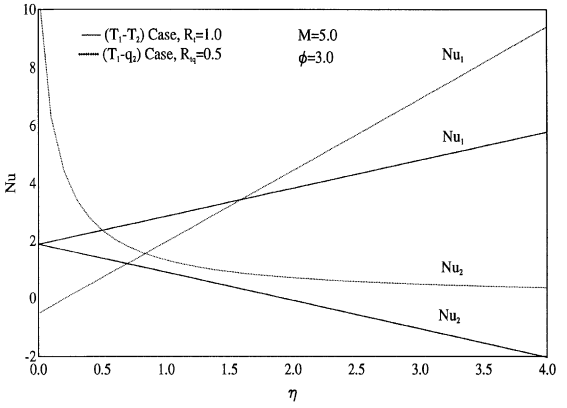

Fig. 14. Effects of Br on Nusselt numbers.

6.2. Hydromagnetic mixed convection flow in a channel with heat generation and viscous and magnetic dissipations

The general Eq. (8) governing the above titled problem does not possess an analytical solution. Therefore, a numerical solution is required. For this reason, the implicit, tri-diagonal finite-difference method discussed by Blottner [6] is employed for this purpose. Eq. (8) is converted into two second-order equations by a change of variable such that $Z = U''$. The resulting equations are then discretised using central-difference quotients. A set of algebraic equations result which can be solved with iterations to deal with the non-linearities of the equations by the Thomas algorithm (see [6]). A

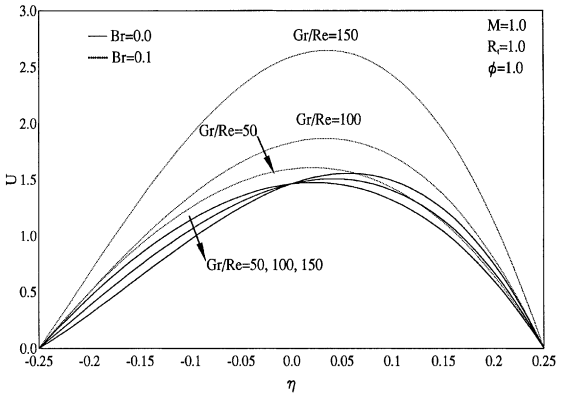

Fig. 15. Effects Br and Gr/Re on velocity profiles for $(T_1 - T_2)$ case.

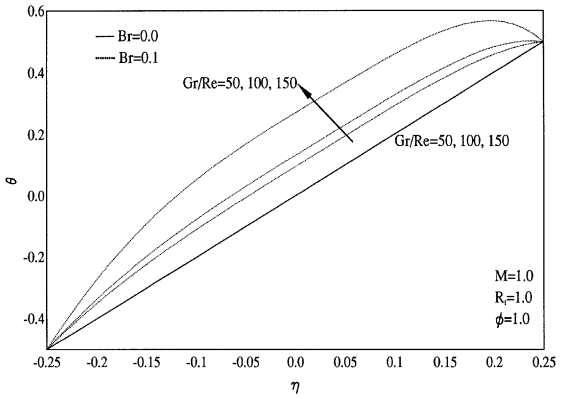

Fig. 16. Effects of Br and Gr/Re on temperatre profiles for $(T_1 - T_2)$ case.

uniform step size of 0.005 is employed to produce the numerical results. The accuracy of the numerical solution is checked against the many analytical solutions reported previously. Only Figs. 15 and 16 are chosen for presentation in this section in order to display the effects of both viscous dissipation and Joule heating on the velocity and temperature profiles in the channel in the presence of buoyancy effects. It is clear from these figures that, for a fixed value of Gr/Re, a larger amount of flow accompanied with a higher thermal state are induced in the channel owing the presence of both viscous dissipation and Joule heating. In addition, the presence of these effects is predicted to be much more pronounced at larger values of Gr/Re.

7. Conclusion

This work focused on the laminar fully developed mixed convective flow of an electrically conducting fluid in a vertical channel in the presence of a magnetic field and heat generation or absorption effects. Three different combinations of thermal left–right wall conditions were prescribed. These thermal left–right wall conditions were isothermal–isothermal, isoflux–isothermal, and isothermal–isoflux conditions. Various analytical solutions for the velocity and temperature profiles for different special cases with the three wall heating conditions were obtained. Also, the heat transfer aspects and the reversed flow conditions were considered and analytical expressions for the Nusselt numbers at the left and right walls of the channel were derived. In addition, analytical solutions for forced convection flow in a channel with both viscous and magnetic dissipations were reported. Finally, the general mixed, convection problem which includes the effects of both viscous dissipation and Joule heating was solved numerically by an implicit finite-difference method. Comparisons with previously published work were performed and found to be in excellent agreement. Graphical results were displayed for selected situations of wall heating conditions and proper conclusions were obtained. It was found that no reversed flow occurs for the case of symmetric channel wall temperatures while reversal flow near the walls is assured for asymmetric channel wall temperatures and mixed isoflux–isothermal or isothermal–isoflux wall thermal conditions. The zone of assured reversal flow was found to increase owing the presence of either of the magnetic field or the heat generation effects or both.

References

[1] W. Aung, G. Worku, Theory of fully developed combined convection including flow reversal, ASME J. Heat Transfer 108 (1986) 485–488.
[2] W. Aung, G. Worku, Developing flow and flow reversal in a vertical channel with asymmetric wall temperatures, ASME J. Heat Transfer 108 (1986) 299–304.
[3] W. Aung, G. Worku, Mixed convection in ducts with asymmetric wall heat fluxes, ASME J. Heat Transfer 109 (1987) 947–951.
[4] W. Aung, Mixed convection in internal flow, in: S. Kakac, R.K. Shah, W. Aung (Eds.), Handbook of Single-phase Convective Heat Transfer, Wiley, New York, 1987 (Chapter 15).
[5] A. Barletta, Laminar mixed convection with viscous dissipation in a vertical channel, Int. J. Heat Mass Transfer 41 (1998) 3501–3513.
[6] F.G. Blottner, Finite-difference methods of solutions of the boundary-layer equations, AIAA J. 8 (1970) 193–205.
[7] A.J. Chamkha, Hydromagnetic three-dimensional free convection on a vertical stretching surface with heat generation or absorption, Int. J. Heat Fluid Flow 20 (1999) 84–92.
[8] K.C. Cheng, R.-S. Wu, Viscous dissipation effects on convective instability and heat transfer in plane Poiseuille flow heated from below, Appl. Sci. Res. 32 (1976) 327–346.

[9] C.-H. Cheng, H.-S. Kou, W.-H. Huang, Flow reversal and heat transfer of fully developed mixed convection in vertical channels, J. Thermophys. Heat Transfer 4 (1990) 375–383.

[10] J.P. Garandet, T. Alboussiere, R. Moreau, Buoyancy driven convection in a rectangular enclosure with a transverse magnetic field, Int. J. Heat Mass Transfer 35 (1992) 741–749.

[11] T.-T. Hamadah, R.A. Wirtz, Analysis of laminar fully developed mixed convection in a vertical channel with opposing buoyancy, ASME J. Heat Transfer 113 (1991) 507–510.

[12] D.B. Ingham, D.J. Keen, P.J. Heggs, Flows in vertical channels with asymmetric wall temperatures and including situations where reverse flows occur, ASME J. Heat Transfer 110 (1988) 910–917.

[13] H.S. Kou, K.J. Lu, Combined boundary and inertia effects for fully developed mixed convection in a vertical channel embedded in porous media, Int. Commun. Heat Mass Transfer 20 (1993) 333–345.

[14] A. Raptis, N. Kafoussias, Heat transfer in flow through a porous medium bounded by an infinite vertical plate under the action of a magnetic field, Energy Res. 6 (1982) 241–245.

[15] E.M. Sparrow, R.D. Cess, Effect of magnetic field on free convection heat transfer, Int. J. Heat Mass Transfer 3 (1961a) 267–274.

[16] E.M. Sparrow, R.D. Cess, Temperature dependent heat sources or sinks in a stagnation point flow, Appl. Sci. Res. A 10 (1961b) 185–197.

[17] L.N. Tao, On combined free and forced convection in channels, ASME J. Heat Transfer 82 (1960) 233–238.

[18] K. Vajravelu, A. Hadjinicolaou, Convective heat transfer in an electrically conducting fluid at a stretching surface with uniform free stream, Int. J. Eng. Sci. 35 (1997) 1237–1244.

[19] K. Vajravelu, J. Nayfeh, Hydromagnetic free convection at a cone and a wedge, Int. Commun. Heat Mass Transfer 19 (1992) 701–710.